Support information for:

Three Dimensional Nanoarchitectures of Co Nanoparticles Inlayed on N-doped Macroporous Carbon as Bifunctional Electrocatalysts for Glucose Fuel Cells

Liangzhen Liu[1, 2], Suqin Ci[1*], Linlin Bi[1,2], JingchunJia, Zhenhai Wen[1, 2, 3*]

1 Key Laboratory of Jiangxi Province for Persistent Pollutants Control and Resources Recycle, Nanchang Hangkong University, Nanchang 330063, China
2 CAS Key Laboratory of Design and Assembly of Functional Nanostructures, Fujian Institute of Research on the Structure of Matter, Chinese Academy of Sciences, Fuzhou, Fujian 350002, P. R. China
3 Fujian Provincial Key Laboratory of Nanomaterials, Fujian Institute of Research on the Structure of Matter, Chinese Academy of Sciences, Fuzhou, Fujian 350002, P. R. China

*E-mail: sqci@nchu.edu.cn, wen@fjirsm.ac.cn

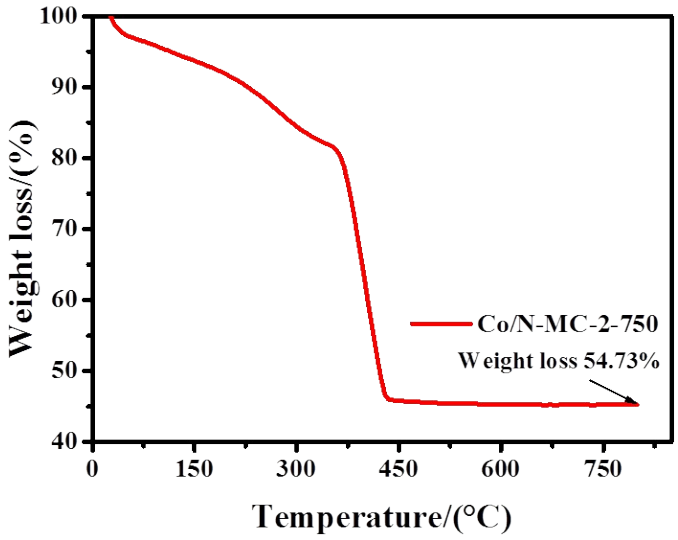

Figure S1. Thermogravimetric analysis curve of Co/N-MC-2-750 measured from 30 to 800 ºC in air atmosphere with a heating rate of 10 ºC/min. It was pointed out that, Co/N-MC-2-750 at between 0 and 100°C, the water was evaporated; between the 200 and 320 ºC, the Co phase was oxidized by air to transform into Co_3O_4 phase; Based on the mass of Co_3O_4 (45.27 wt%) left after 800 ºC, it can be calculated that the Co content in hybrid is 61.86 wt%.

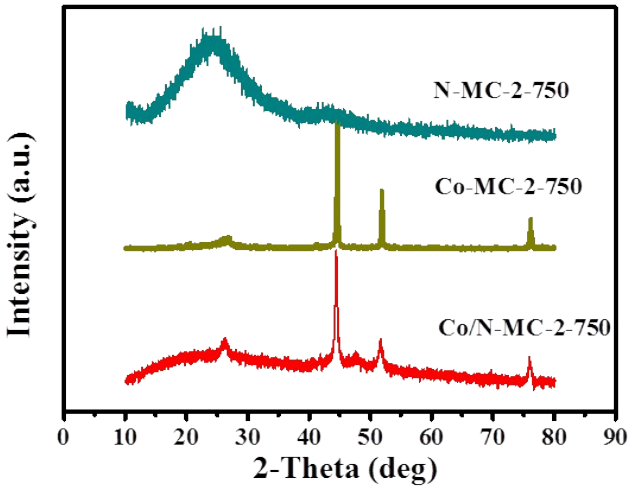

Figure S2. XPS spectra of Co/N-MC-2-750, Co-MC-2-750 and N-MC-2-750.

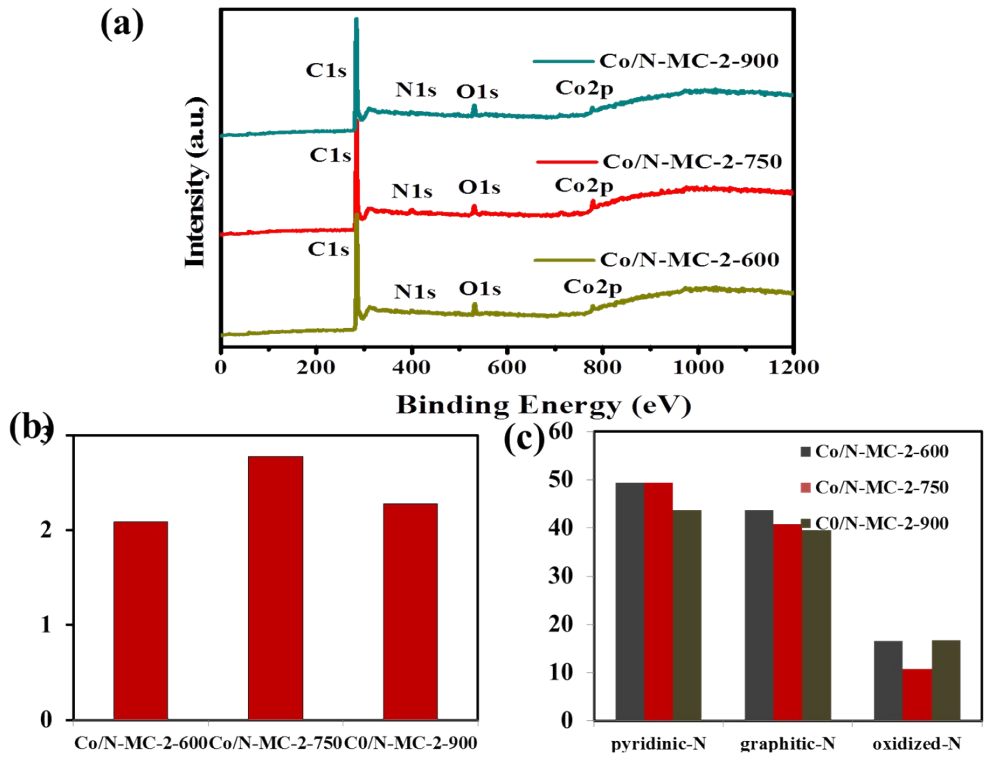

Figure S3. (a) XPS surveys of the Co/N-MCs samples; (b) the total N content (percentage content: 100 %) of the all Co/N-MCs samples; (c) different types of N in Co/N-MC-2-600, Co/N-MC-2-750 and Co/N-MC-2-900.

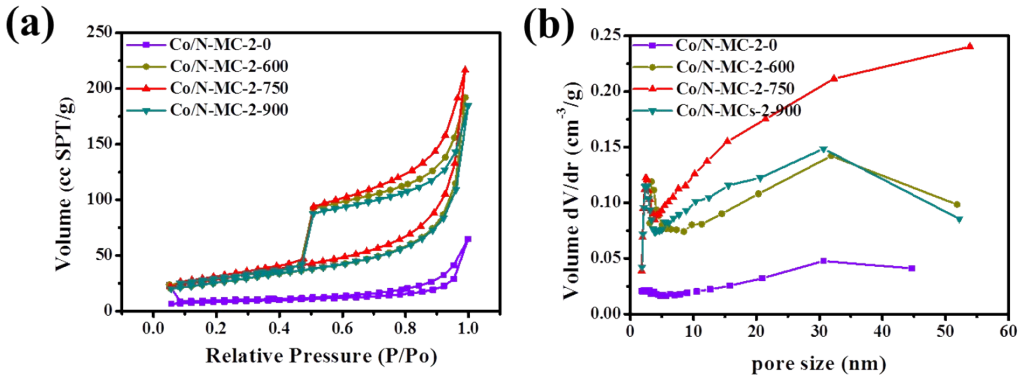

Figure S4. (a) N_2 adsorption/desorption isotherm curves of all catalysts and (b) pore size distributions of all Co/N-MCs catalysts.

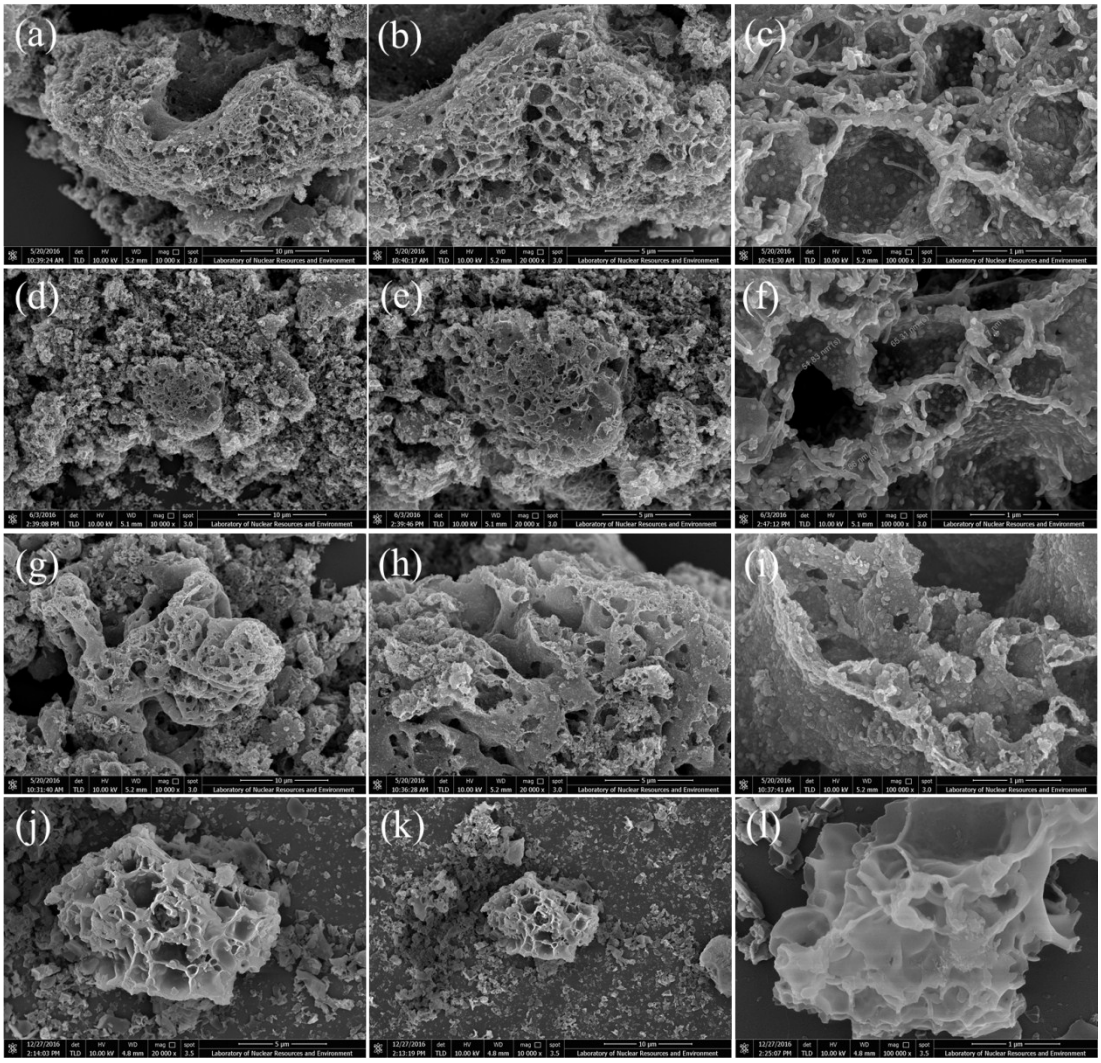

Figure S5. The SEM images of Co/N-MC-2-750 (a, b, c); Co/N-MC-2-900 (d, e, f), Co/N-MC-2-600 (g, h, i) and Co/N-MC-2-0 (j, k, l), respectively.

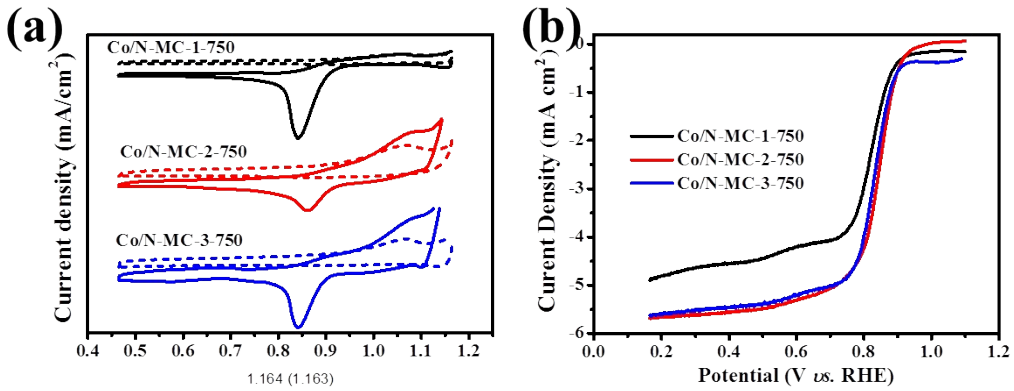

Figure S6. (a) Cycle voltammetry of Co/N-MC-1-750, Co/N-MC-2-750， Co/N-MC-2-750 and Co/N-MC-3-750 in O_2 (the solid line) and N_2 (the dotted line) saturated 0.1M KOH solution with a scanning rate of 10 mV s^{-1}; (b) linear sweep voltammetry of Co/N-MC-1-750, Co/N-MC-2-750 and Co/N-MC-3-750 at a rotation rate of 1600 rmp.

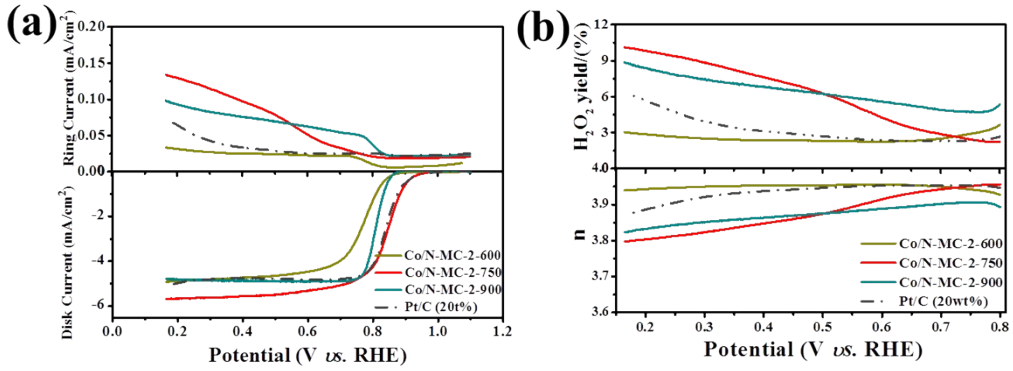

Figure S7. (a) RRDE curves of various electrocatalysts in 0.1M KOH solution at a rotation speed of 1600rmp: current density at disk and ring electrodes for Co/N-MC-2-600, Co/N-MC-2-750, Co/N-MC-2-900 and Pt/C (20wt%); (b) H_2O_2 yield and electron transfer number (n) for Co/N-MC-2-600, Co/N-MC-2-750, Co/N-MC-2-900 and Pt/C (20wt%).

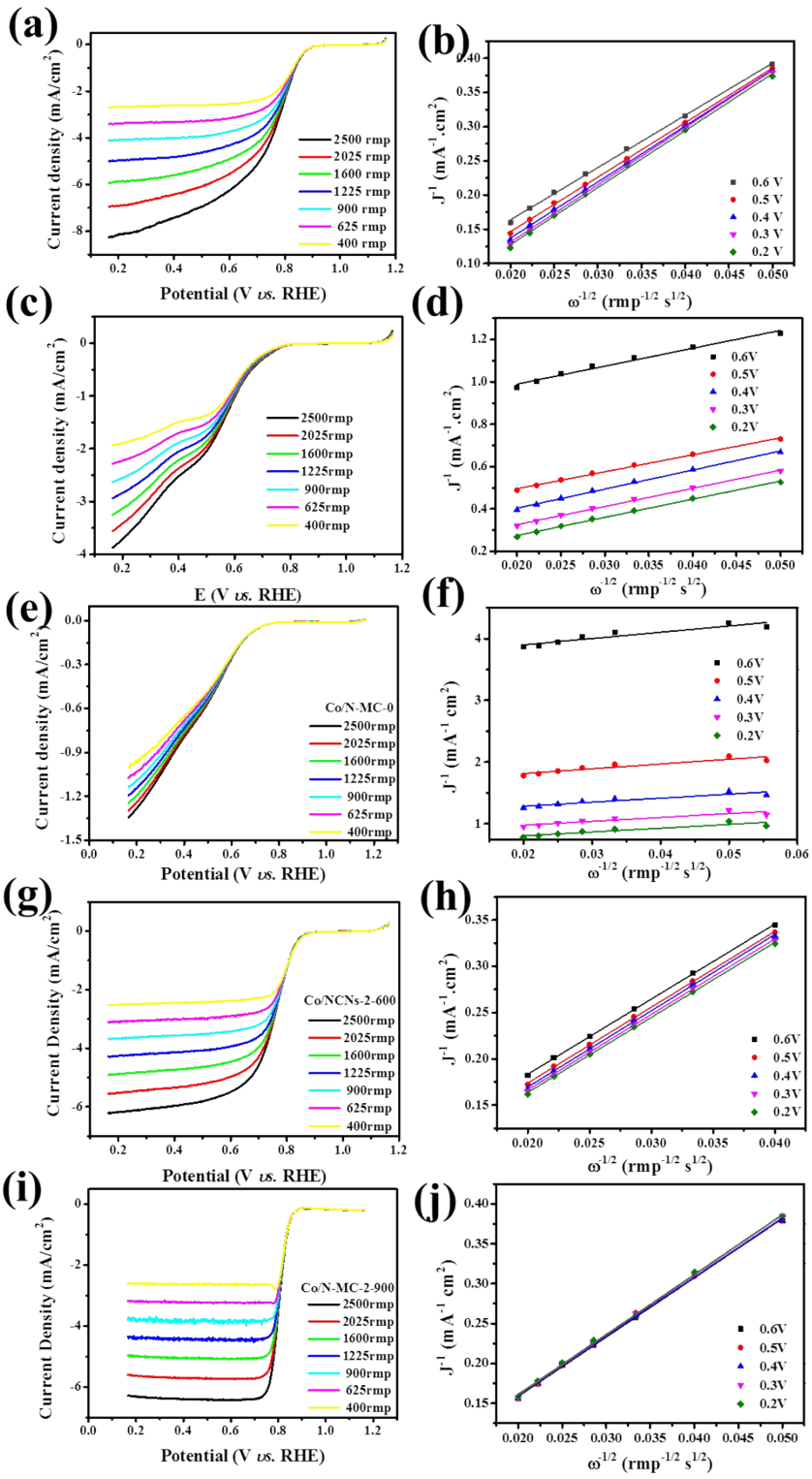

Figure S8. Rotation disk electrode (RDE) polarization curves of the N-MC-2-750 (a), the Co-MC-2-750 (c), the Co/N-MC-2-0 (e), the Co/N-MC-2-600 (g) and the Co/N-MC-2-900 (i) at various rotating speeds, respectively; the corresponding K-L plots of the N-MC-2-750 (b), the Co-MC-2-750 (d), the Co/N-MC-2-0 (f), the Co/N-MC-2-600 (h) and the Co/N-MC-2-900 (j) at different potentials, respectively.

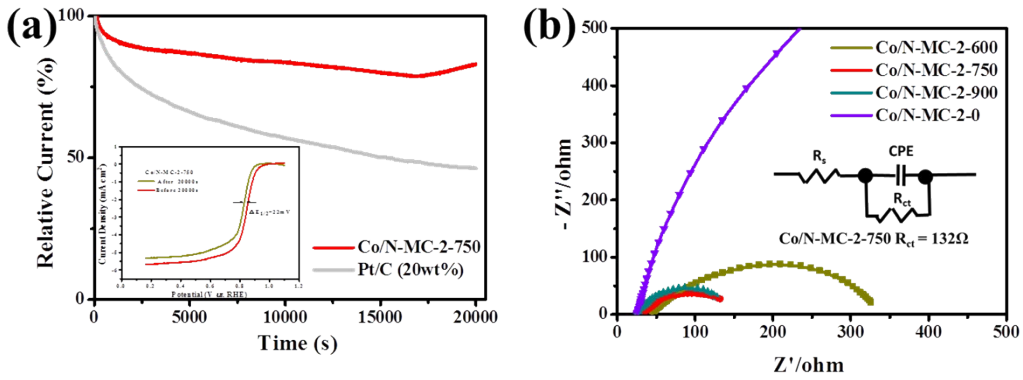

Figure S9 (a) Chronoamperometry of Co/N-MC-2-750 and Pt/C electrodes in O_2-satureted 0.1M KOH at -0.3V(*vs. Ag/AgCl*) for 20,000 s (Inset shows RDE polarization curves of Co/N-MC-2-750 of before i-t test and after i-t test); (b) Impedance diagram of all Co/N-MCs catalysts in oxygen saturated 0.1 M KOH electrolyte at a rotation rate of 1600 rpm.

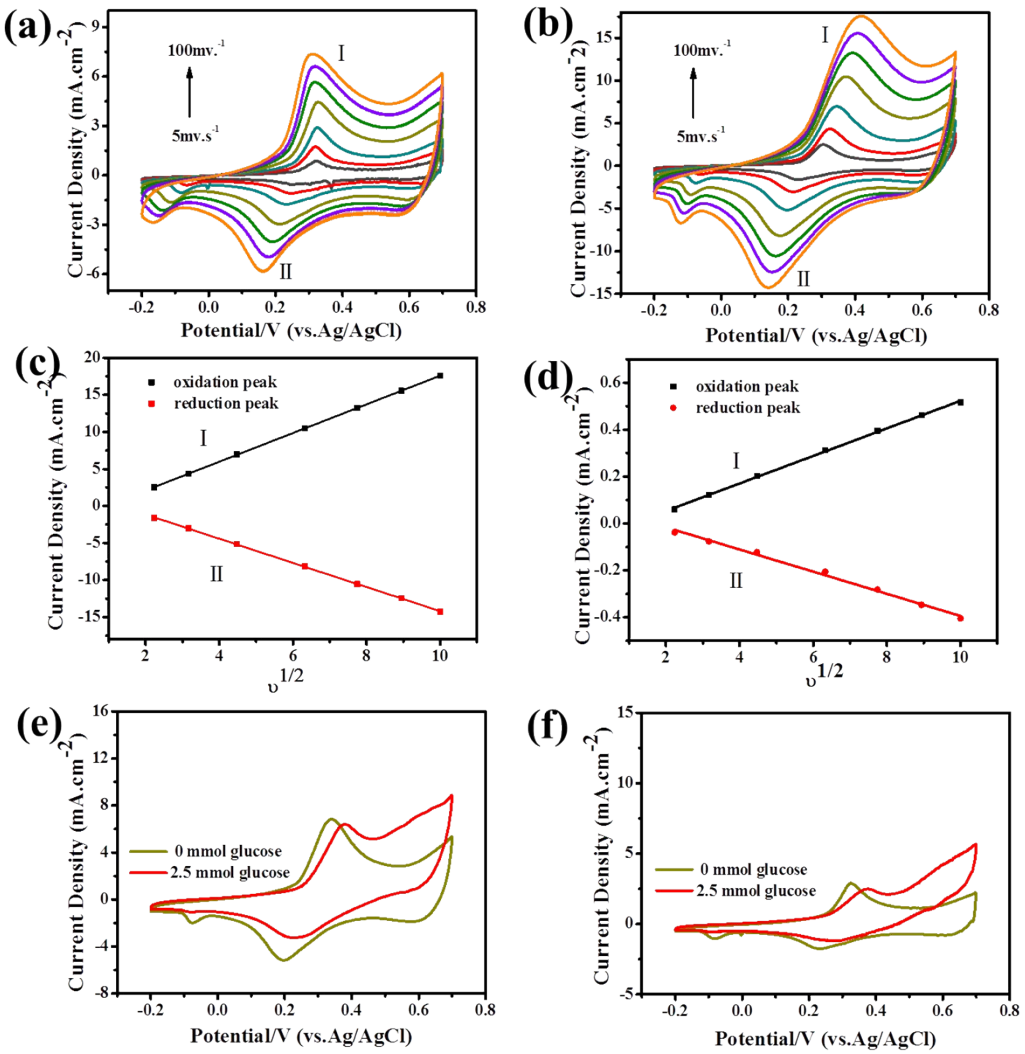

Figure S10. (a, b) CVs of the Co/N-MC-2-600 and Co/N-MC-2-900 in Ar-saturated 0.1 M KOH solution at various scan rates of 5, 10, 20, 40, 60, 80, 100 mV/s; (c, d) the plot of peak currents of the Co/N-MC-2-600 and Co/N-MC-2-900 *vs.* square root of scan rate; (e, f) CVs of the Co/N-MC-2-600 and Co/N-MC-2-900 in absence and presence of 2.5 mM glucose at a scan rate of 100 mV s^{-1} in Ar-saturated 0.1 M KOH solution.

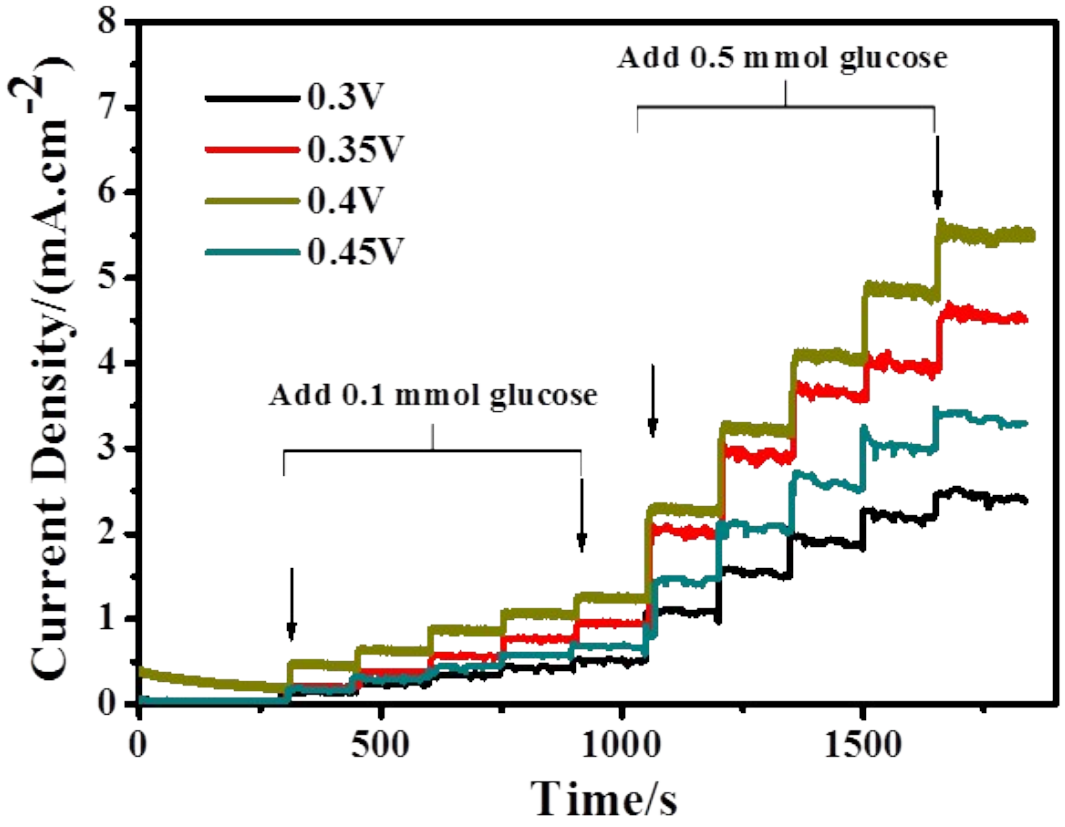

Figure S11. (a) Amperometric response to successive additions of glucose at the Co/N-MC-2-750 electrode in Ar-saturated 0.1M KOH solution with magnetic stirring at different applied potential.

Table S1. The detailed electrochemical performance parameters of all catalysts and the Pt/C (20 wt%) catalyst for ORR, and the other corresponding experimental data.

Sample	E_{onset} (V)	$E_{1/2}$ (V)	E_{cp} (V)	J_k (mA cm^{-2}) at 0.5V	n	the Tafel plots	BET surface area ($m^2.g^{-1}$)	Pore Volume ($cm^3.g^{-1}$)
Co/NCNs-0	0.823	0.465	0.609	-	-	-	28.1	0.097
Co/NCNs-600	0.904	0.77	0.78	4.87	3.93-3.95	72.75	92.36	0.30
Co/NCNs-750	1.000	0.84	0.863	6.25	3.80-3.96	61.45	103.4	0.34
Co/NCNs-900	0.906	0.809	0.839	5.38	3.82-3.91	47.36	92.5	0.29
Pt/C (20%)	0.992	0.839	0.871	-	3.88-3.95	75.66	-	-

Table S2. Comparisons of the ORR performance between this work with representative published data on M, N - double doped carbon materials.

M-N-C material	Onset potential (V vs RHE)	Half-wave potential (V vs RHE)	Average electron transfer number (n)	BET surface area ($m^2.g^{-1}$)	Reference
Co/NG	0.963	0.814	3.8	65.1	5
Co,N-CNF	0.889	0.809	0.78	1170	12
Co-C@Co_9S_8 DSNCs	0.96	0.83	~3.8	106.2	2
Fe-NMCSs	1.027	0.86	3.94~3.99	674	50
NCNTFs	0.95	0.87	3.97~3.99	513	10
Fe-NG	0.885	0.752	-	1200	38
Co-N-GCI	~0.97	0.857	~3.9	365.2	21
GMP-CoPors	~0.95	0.818	3.8	685	20
PANKCo2	~0.92	0.839	3.6~.61	-	18
FeCo–NMCG	0.904	0.774	3.95	371	24
Fe-N/C-700	0.956	0.84	4.02	363	55
Co-N-OMMC-0.6	~0.97	0.83	3.9	635	56
Co/N/GR	0.897	~0.8	3.9	186	43
Co/CoNx/CNT	0.9	0.77	3.77	138.9	44
NCN-Co-0.1	0.961	0.824	3.85~3.99	-	45
Co/N-MC-2-750	1.0	0.84		103.5	This work

Table S3. Impedance components determined by fitting the experimental data using the equivalent circuit (Figure S9b). (Rs represent electrolyte resistance; Rct the charge transfer resistance； CPE represent interfacial resistance.)

Sample	Rs	Rct	CPE-T	CPE-P
Co/N-MC-0	25.41	2903	0.0000082	0.89796
Co/N-MC-600	43.9	308.6	0.0001251	0.64386
Co/N-MC-750	31.82	132.5	0.0010454	0.64761
Co/N-MC-900	26.23	124.2	0.0009128	0.80128
Anode (GFC)	0.20	1.87	0.000159	0.82327
Cathode (GFC)	13.26	16.42	0.0000926	0.8102